*SATTLER, WORCHESKY, RITTER,
SIMONIS & RIESSLER

INFRARED DIAGNOSTICS FOR NEAR-MILLIMETER WAVE SOURCES

JOSEPH P. SATTLER, Ph.D., TERRANCE L. WORCHESKY, KENNETH J. RITTER,
GEORGE J. SIMONIS, Ph.D. and WALTER A. RIESSLER, Ph.D.
U.S. ARMY ELECTRONICS RESEARCH AND DEVELOPMENT COMMAND
HARRY DIAMOND LABORATORIES
ADELPHI, MD 20783

JUN 1978

11 p.

The near-millimeter wave (NMMW) region of the electromagnetic spectrum may be defined as that region between 3.2 and 0.3 mm in wavelength (or equivalently between 94 and 1000 GHz, or between 3.1 and 33.3 cm^{-1}). This region near 1 mm is considered to be a unique region because its components and techniques are hybrids of the microwave and infrared (IR) regions that bracket it and because its atmospheric transmission windows permit reasonable propagation under adverse conditions. The justifications for military consideration of NMMW systems involve complex technical questions (1). Briefly stated, they arise from requirements for various "imaging" and radar systems which can operate under all weather conditions and the environment of battlefield smokes and dust. With a judicious balance of parameters, NMMW systems can combine the propagation advantages of the microwave region with high resolution that is characteristic of IR and optical systems.

This paper reports on new systematic diagnostic procedures developed in part at The Harry Diamond Laboratories (HDL) for obtaining the basic molecular information necessary for modeling and scaling the operation of known photon-pumped NMMW sources and for prediction of new NMMW emission and associated pump frequencies. Our procedures involve the use of tunable IR diode lasers to reveal important details of previcusly unresolved molecular absorption lines. The sub-Doppler-width resolution achievable with these lasers has permitted us to extend into the IR region a combination of accurate heterodyne and Stark absorption techniques previously employed routinely only in microwave spectroscopy.

First, the basic physics of photon-pumped NMMW sources is explained. Then the instrumental configurations involving the frequency

DISCLAIMER NOTICE

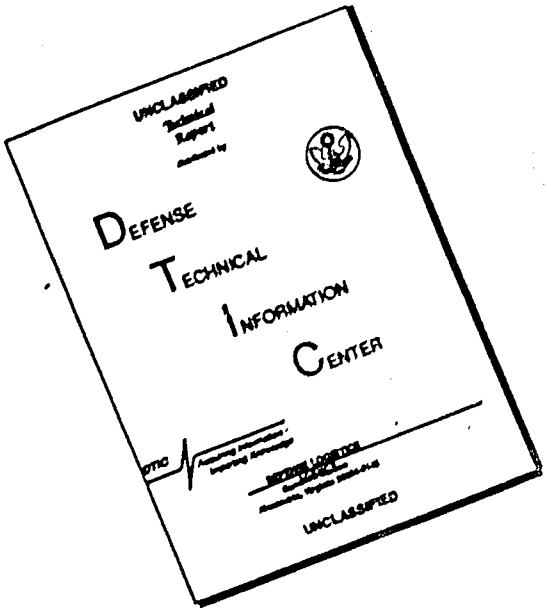

THIS DOCUMENT IS BEST QUALITY AVAILABLE. THE COPY FURNISHED TO DTIC CONTAINED A SIGNIFICANT NUMBER OF PAGES WHICH DO NOT REPRODUCE LEGIBLY.

*SATTLER, WORCHESKY, RITTER
SIMONIS & RIESSLER

tunable lead-salt (PbSnSe) diode laser are discussed, with emphasis on heterodyne and Stark spectroscopic techniques used at HDL. The results obtained from studies of CH_3F, D_2O, and CH_3OH are presented, and the relationships to NMMW generation are given. New NMMW frequencies in atmospheric windows are predicted.

Photon-Pumped NMMW Sources

Photon-pumped NMMW sources operate on the principle of obtaining stimulated emission at a NMMW frequency in a gaseous molecular medium. The NMMW output frequency may result from a laser population inversion emission or a Raman emission. In either case, as illustrated in Fig. 1, it is necessary to find an IR emission transition, hν, which closely matches the molecular absorption energy, $E_2 - E_1$. The frequency separation between pump and absorption should be within about 1 GHz for pulsed NMMW output and within 100 MHz for cw NMMW output.

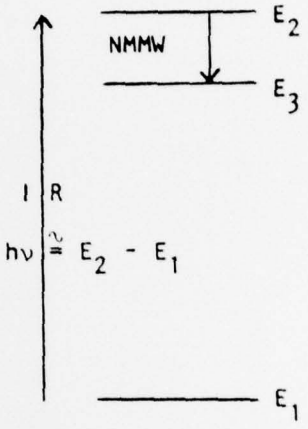

Fig. 1. NMMW Photon pumping scheme.

Conventional grating spectrometers do not have adequate resolution to determine accurately the frequency separation of the pump emission and IR absorption. However, tunable IR diode lasers, with a resolution over 20 times that of conventional spectrometers, can resolve IR spectral lines to less than their Doppler width, which is typically between 50 and 100 MHz for IR molecular transitions near 10 μm (1000 cm^{-1} or 30 x 10^{12} Hz). This is illustrated in Fig. 2. The upper portion shows the survey scan spectrum obtained with a conventional spectrometer for the gas CH_3F at a pressure of a few torr (2). The lower inserted oscillographs give our results obtained with lead-salt diode lasers. In these oscillographs, the upper traces correspond to the CH_3F absorption versus frequency, and the high resolution of the diode laser much detailed absorption structure is displayed where only singlet or blended band structure occurs in the conventional spectrum. The regularly spaced near-sinusoidal lower traces in the oscillographs correspond to periodic transmission maxima spaced by 1475 MHz (0.0492 cm^{-1}); these curves result from the variations with diode laser frequency of transmission through a Ge bar, and are used to calibrate the frequency scale.

A complete understanding of a photon-pumped NMMW source requires (a) identification of the quantum numbers associated with the molecular transitions; (b) measurement of the frequency difference between

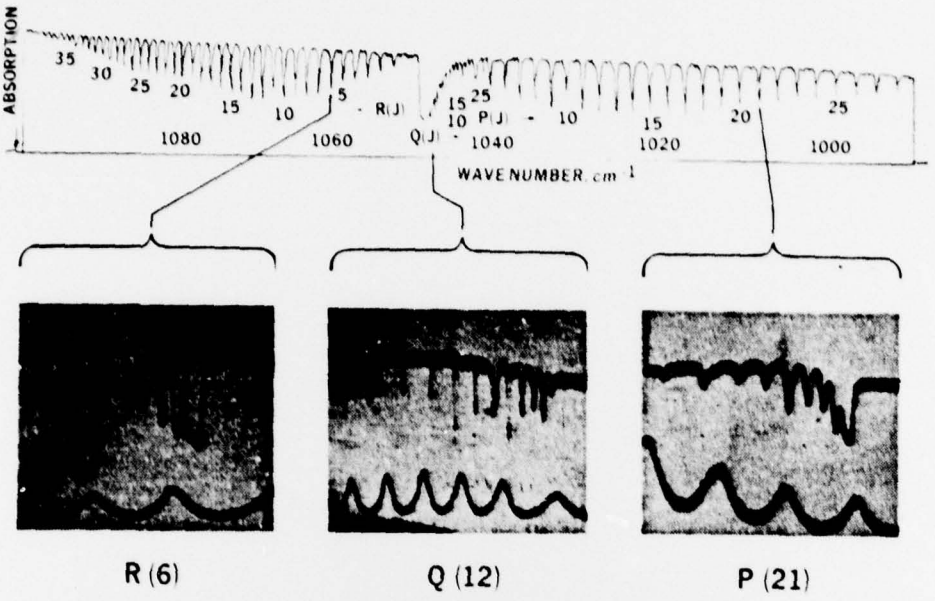

Fig. 2. Comparison of conventional spectrum (upper trace) and tunable diode laser spectra (lower traces) for CH_3F.

photon pump and molecular absorption; (c) measurement of IR line shapes, line strengths, transition rates, and pressure broadening effects; (d) related conventional molecular spectroscopy; (e) related NMMW spectroscopy. Our IR measurements have involved the first three items, and we have drawn from other publications for the other information. The rest of this paper describes our techniques and the application of our results to the molecular transitions of NMMW sources.

Diode Laser Spectrometer

Our first diagnostic step in studying a NMMW gas was to obtain the ultrahigh resolution IR spectrum in the region of interest. This procedure usually revealed important features of previously unresolved absorption line structure. The results of conventional spectroscopy often provide useful experimental and theoretical guides as to what one may expect. Indeed the operation of the diode laser may be compared with the operation of a microscope with very high resolution; without conventional low magnification information, it may be impossible to interpret the high-resolution structure.

The diode laser spectrometer is shown in Fig. 3. The lead-salt diode laser was fabricated by Laser Analytics and typically produced several hundred microwatts of power in each of about six principal

simultaneously oscillating laser modes when operating on a liquid-He cold finger. Varying the injection current between 0.23 and 2.0 A resulted in a piecewise tunability between 1005 and 1020 cm^{-1} at liquid-He temperature. The continuous tuning range of a given mode was about 0.3 cm^{-1} under these conditions. However, the useful diode-laser tuning range was extended by 140 cm^{-1} to higher frequencies by allowing the liquid-He to evaporate and the dewar to warm up slowly, or by mounting the diode in a closed-cycle variable-temperature cryogenic refrigerator. The refrigerator kept the diode laser at temperatures between 10 and 77 K with a short term stability better than 3×10^{-4} K. These temperatures allowed the diode laser to be coarsely tuned from 1030 to 1160 cm^{-1}. By adjusting the laser current, the frequency could be fine tuned at the rate of 10 MHz/mA. As the temperature was increased, the threshold current also increased, and fewer modes operated, but the current tuning range of these modes increased to about 1 cm^{-1}.

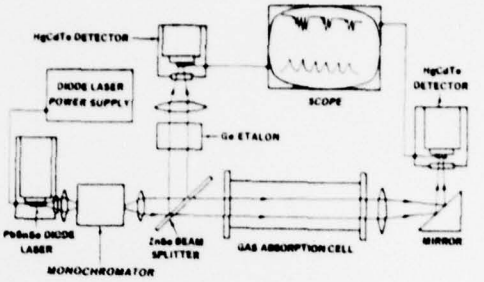

Fig. 3. Schematic diagram of diode laser spectrometer.

The radiation from the diode laser was first passed through a ¼-m monochromator used as a narrow band-pass filter to select a principal laser mode. A beam splitter then passed one portion of the radiation through a Ge bar etalon employed for the calibration of optical frequency differences, while the second portion of the radiation passed through the gas absorption cell (3). Two separate HgCdTe detectors simultaneously received the radiation passed through the etalon and the gas cell. Typically, a sawtooth current ramp of about 0.1-A amplitude with a frequency of about 100 Hz was applied to the diode laser to sweep its output frequency. Direct video presentation of the molecular absorption and the etalon channel spectrum was given simultaneously on a dual-beam oscilloscope for the warm-up exepriments. When the diode was mounted in the cryogenic refrigerator, a chopper and lock-in amplifiers were used to present the molecular and etalon channel spectra versus diode laser current on an X-Y-Y' recorder. Absorption-line separations were measured by comparison with the periodicity (1475 MHz) produced by the etalon. The gas sample cell was 30 cm long. Measurements were made at various pressures between 0.1 and 10 torr.

The search for a particular molecular absorption line proceeded in the following manner. As the diode laser temperature slowly increased, a manual scan of current between 0.2 and 2 A was repeatedly

made. The sawtooth ramp also was applied, and wide spectrometer slits were used during the search. Narrow slits were then inserted to discriminate against unwanted laser modes when it was desired to confirm the appearance of a particular absorption line, and the sawtooth ramp amplitude was decreased for better resolution.

As an example of the results obtainable with the diode laser spectrometer, Fig. 4 shows the tracings obtained from the plotter output of the 12 lines of the Q(J = 12, K) multiplet of CH_3F. This is similar to an oscillograph in Fig. 2, except that in this figure the frequency scale is more linear and increases toward the right.

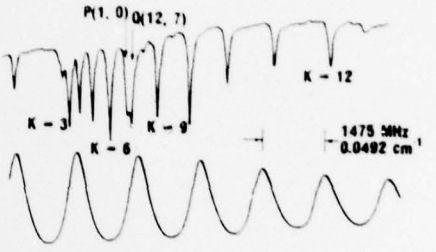

Fig. 4. Absorption spectrum of ν_3, Q(J = 12, K) transitions of CH_3F (upper trace) and etalon channel spectrum (lower trace).

Diode Laser Heterodyne Spectrometer

Although the experimental arrangement discussed above can provide remarkable sub-Doppler IR resolution, it cannot be used to measure the frequency difference between a molecular absorption and the photon-pump laser emission transition which must be obtained for NMMW diagnostics. Since the pumping laser is usually a CO_2 laser, and since the frequencies of this laser have been measured to high accuracy, a beat-note or heterodyne measurement of the pump laser with the diode laser frequency centered at a molecular absorption can determine the absolute frequency of the molecular absorption. Fig. 5 is a schematic of the experimental arrangement used at HDL. Information regarding previous related experimental procedures may be found in Refs. (4) and (5). For heterodyne measurements, the diode laser was mounted in the cryogenic refrigerator. As before, fine tuning was done by adjusting the injection current. The diode laser output was externally chopped and sent to a beamsplitter. Approximately 60% of the radiation passed through a monochromator to eliminate all but one longitudinal mode. The output radiation was made to pass through the gas cell and then onto the HgCdTe detector. The detected absorption signal was

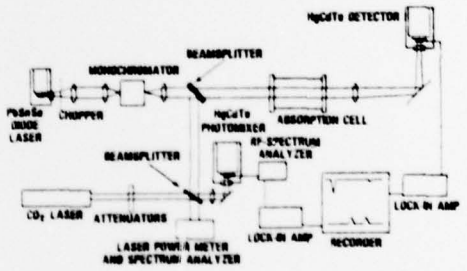

Fig. 5. Schematic diagram of diode laser heterodyne spectrometer.

fed into a lock-in amplifier, and its output was fed into the Y channel of an X-Y-Y' recorder whose X axis was driven as a linear function of the slowly changing diode-laser tuning current. The other portion of the diode-laser radiation was sent to an SAT Model C1 HgCdTe photomixer (3 dB bandwidth of 150 MHz) and heterodyned against a local oscillator.

The local-oscillator laser was a Sylvania Model 950 CO_2 laser whose frequency could be adjusted to be close so that of the molecular absorption line by use of an intracavity diffraction grating. The laser was set to line center maximizing the output power with a piezoelectric transducer. Although the gain profile and thus the absolute laser frequency are uncertain because of the pressure of the lasing gas mixture, this uncertainty is less than 2 MHz (6). The short-term frequency stability of this CO_2 laser was measured to be better than 1 MHz for periods of several minutes.

The rf signal from the photomixer was amplified by a low-noise, wideband amplifier and was detected with an HP model 141T spectrum analyzer system operating as a narrow-band (300-kHz) fixed-frequency receiver, tunable between 0 and 1.2 GHz. Video output at the chopping frequency was detected with a second lock-in amplifier whose output was applied to the Y' channel of the recorder. As the diode-laser frequency was tuned toward the CO_2 laser frequency, the beat note frequency decreased. When this frequency equaled the preset spectrum analyzer detection frequency, a marker was produced in the Y' channel. After the diode-laser frequency passed through the CO_2 laser frequency and their difference again equaled the setting of the spectrum analyzer detection frequency, another marker was generated. Thus we could measure the frequency difference between CO_2 laser line and a molecular absorption line by comparing the absorption and marker traces of the recorder.

Fig. 6 shows the result of one experimental run for D_2O. The upper trace shows the output from the detector that measured the absorption of the diode laser radiation by the D_2O gas; the lower trace shows the frequency markers generated by the heterodyne system. This run was for the absorption $6_6 \rightarrow 5_4$, $6_5 \rightarrow 5_5$ and $7_{-1} \rightarrow 6_{-3}$ near the 9P32 CO_2 laser line. High-resolution grating spectroscopy had placed the $7_{-1} \rightarrow 6_{-3}$ absorption 1770 MHz above the $6_6 \rightarrow 5_4$, $6_5 \rightarrow 5_5$ absorption (7). In Fig. 6, the $6_6 \rightarrow 5_4$, $6_5 \rightarrow 5_5$ absorption is 1177 MHz below the

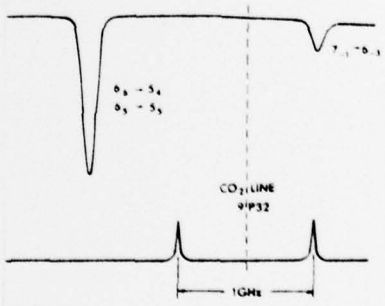

Fig. 6. D_2O absorption (upper trace) and frequency markers (lower trace).

CO_2 laser line, while the $7_{-1} \rightarrow 6_{-3}$ absorption is 565 MHz above this line. To reduce errors arising from the nonlinear tuning of frequency with current, we subsequently produced markers slightly below and slightly above each absorption line by changing the spectrum analyzer detection frequency by 100 MHz during each run. With these 100-MHz markers bracketing each absorption, we interpolated over 100 MHz to find the absorption frequency and thus avoided extrapolations over several hundred megahertz.

We checked the frequency calibration of this system by comparing our data with high resolution data taken by other complex spectroscopic techniques. These included not only the $5_0 \rightarrow 4_0$ transition of D_2O, but also several lines in CH_3F (8). Fig. 7 shows heterodyne results from the Q(12, K) transition of CH_3F. By interpolation, the CO_2 laser 9P20 line lies 53 MHz above the Q(12, 1) and 51 MHz below the Q(12, 2), in agreement with previous results (8). The error in our measurements is ±15 MHz (±0.0005 cm^{-1}). The frequency instability of the diode laser caused by the mechanical and thermal fluctuations of the refrigerator comprises the largest contribution to this uncertainty.

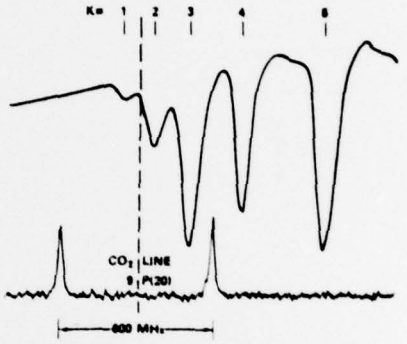

Fig. 7. Heterodyne spectroscopy of ν_3, Q(J = 12, K) transitions in CH_3F.

Diode Laser Stark Spectrometers

The application of external electric fields to gaseous molecules is common in microwave absorption spectroscopy where the high resolution of microwave components permits detection of small changes in transition frequency caused by the Stark effect (9). Although Stark fields have been used to tune IR molecular absorption frequencies through nearby laser line frequencies, until the present work, no publication has reported entire resolved Stark components in IR absorption spectroscopy.

A Stark gas absorption cell was constructed with metal plates 10 cm wide by 36 cm long separated by 0.203 cm. This cell could be substituted for the gas cells in the experimental arrangements depicted in Fig. 3 and 5. The usefulness of the Stark effect arises from the ability to assign directly and unambiguously the quantum numbers corresponding to a molecular transition from the pattern of new absorption lines which result when the electric (E-) field is applied.

*SATTLER, WORCHESKY, RITTER, SIMONIS, & RIESSLER

In Fig. 8 is shown the observed structure obtained when static E-fields were applied to a ν_4, R(J = 2, K = 2) transition in CH_3OH with $\vec{E}$ first parallel, then perpendicular to the linear polarization of the diode laser radiation. The quantum numbers, K, corresponding to the projection of the rotational quantum number, J, on the "symmetry" axis of the molecule, could be readily assigned since K = 0 lines showed no resolvable Stark splittings, whereas other lines showed well-resolved linear or quadratic Stark effects. Stark effects in CH_3OH and CH_3F have been studied and are discussed below.

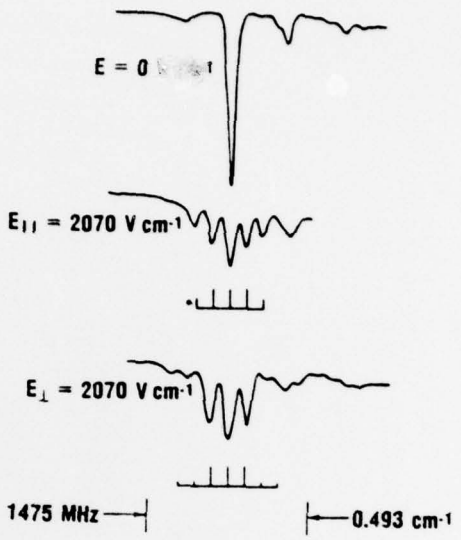

Fig. 8. Linear Stark effect on ν_4, R(J = 2, K = 2) transitions in CH_3OH showing observed and calculated patterns.

Spectroscopy of CH_3F

Methyl fluoride is considered to be an important NMMW and submillimeter wave (SMMW) molecule because strong (13 mW cw and 10 kW pulsed) output power is obtainable at 0.496 mm wavelength. This radiation is given off when the ν_3, Q(12, K = 1,2) transitions depicted in Fig. 2, 4, and 7 are pumped by the 9P20 line of a CO_2 laser (10).

We made a detailed examination of the Q branch of the ν_3 fundamental band of CH_3F (11). Fig. 9 shows typical dual-beam oscilloscope traces. The lower trace contains the regularly spaced maxima and minima of the etalon channel spectrum. The upper trace displays the K-structure of the Q(J, K) absorption lines for J = 3 to 6. These lines are identified according to the symmetric top model where the quantum number J refers to the rotational angular momentum and the axial quantum number K is the projection of J on the C-F symmetry axis. For Fig. 9 and 10, frequency increased toward the right and gas pressure was about 0.5 torr. Some nonlinearity in the diode laser frequency ramp occurred at the start of each application of the sawtooth current ramp (toward the left of the figures); also, there were flyback discontinuities (at the edges of each trace). A better resolved picture of the Q(5, K) quintet appears in Fig. 10, and pictures of the Q(12, K) multiplet appear in Fig. 2, 4 and 7.

The extra line near the Q(12, 7) line is the P(1, 0) line. This has been verified by a Stark measurement. The P(1, 0) line undergoes

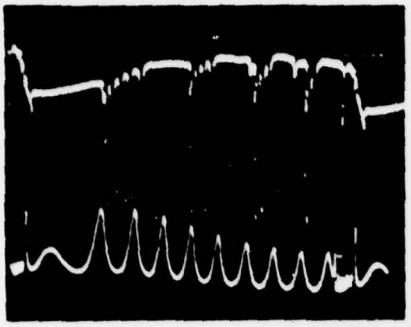

Fig. 9. Diode laser scan over region of several Q(J, K) lines.

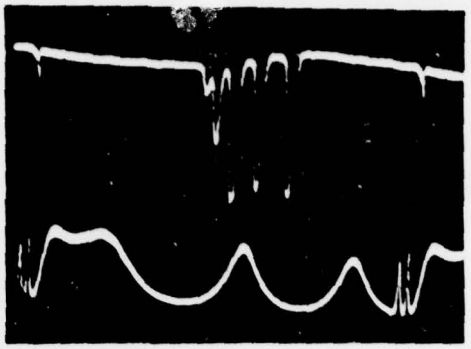

Fig. 10. Diode laser scan of Q(J = 5, K) quintet.

a quadratic Stark shift and has been found to be shifted by -50 MHz with application of a Stark field of 2241 Vcm^{-1}, in excellent agreement with our calculated shift of -48 MHz. Assignment of the symmetric top quantum numbers J and K is particularly easy for lines with $J \leq 12$ in the Q branch because the intensities generally follow the Honl-London intensity rules (12), and most of the lines are well separated with J lines corresponding to the K-values being visible in each multiplet. The K = 1 line is at the lowest frequency of the J multiplet, and lines of increasing K-value appear at correspondingly increasing frequencies. Also, lines with K-values that are evenly divisible by three are stronger than adjacent lines in accordance with the statistics arising from nuclear exchange symmetry (12). As J increases, the strengths of the K = 1 and 2 lines diminish, and the varying intensities help to confirm the line assignments.

We have also obtained spectra of several P- and R-branch lines. In accordance with the Honl-London intensity rules, the lines of low K are of greater intensity than the high-K lines in a J multiplet. It appears that the low-K lines, especially K = 0 and 1, are less than a line width apart, and therefore only J - 1 distinct lines appear for the P branch, and J distinct lines appear for the R branch for J > 0. This behavior is consistent with the spectra calculated from reported values of the vibration-rotation parameters and with line assignments based on the increased strength of lines with K evenly divisible by three. In the P and R branches, as in the Q branch, the frequency increases with increasing value of K.

In Table I are presented the measured and calculated widths of the Q-branch multiplets. The width of each J multiplet has been

*SATTLER, WORCHESKY, RITTER,
SIMONIS, RIESSLER

Table I. Frequency Separation Between Q(J, K = J) and Q(J, K = 1) Lines

J	Measured Separation (MHz)	Calculated Separation[a] (MHz)
2	137 ± 30	133 ± 2
3	386 ± 30	355 ± 10
4	749 ± 40	664 ± 28
5	1081 ± 60	1061 ± 66
6	1581 ± 60	1546 ± 134
7	2204 ± 90	2121 ± 247
8	2836 ± 30	2784 ± 418
9	3636 ± 110	3538 ± 666
10	4543 ± 110	4384 ± 1011
11	5578 ± 110	5324 ± 1475
12	6680 ± 110	6358 ± 2083

Table II. Frequency Separation Between Q(J, K = 1) and Q(J = 1, K = J + 1) Lines

J	Measured Separation (MHz)	Calculated Separation[a] (MHz)
1	1189 ± 100	1221.5 ± 2.5
2	1677 ± 100	1677 ± 9
3	2000 ± 100	2045 ± 29
4	2351 ± 100	2224 ± 67
5	2582 ± 100	2514 ± 135
6	2526 ± 100	2615 ± 248
7	2500 ± 100	2625 ± 419
8	2415 ± 100	2544 ± 667
9	2298 ± 100	2370 ± 1010
10	1983 ± 100	2101 ± 1480
11	1680 ± 100	1736 ± 2080

[a]Calculated with parameters in Ref. (11).

measured as the separation between the K = J and K = 1 components. In a similar manner, Table II gives the separation of adjacent multiplets. No attempt has been made to extract best-fit constants from our data on inter- and intra-multiplet line separations. Our experimental errors of about 100 MHz are caused in part by the low finesse of the etalon, by laser radiation of nearby parasitic modes, and by changes in the laser power output and tuning rate with current. The increasingly large errors in the calculated separations occur because the vibration-rotation parameters that are not well known are multiplied by big integers for large values of J and K, thus increasing the relative error. For example, the calculation of the positions of the P(1, 0) and Q(12, 7) lines, which appear close together in Fig. 4, is not reliable enough to distinguish the lines. Nevertheless, the diode laser spectrum consisting of regularly increasing spacings of the Q(12, K) lines indicate that the Q(12, 7) line should be at a higher frequency than the P(1, 0) line. This information is consistent with our Stark experiment.

The agreement between our measurements and the calculated spectra is within experimental error, except for the Q(4, K) multiple where the measured width seems slightly large. For low values of J and K, the line separations obtained by using the published values of the vibration-rotation parameters are believed to be about two orders of magnitude more accurate than we can measure with the diode laser.

This accuracy is not surprising since the experiments (8) and (13) have encompassed a large number of very accurate data relating to lines of low J- and K-values in the immediate vicinity of available CO_2 laser lines. Nevertheless, the diode laser is very useful for those regions of the spectrum where it is not possible to extrapolate the results of other experiments. Our recent calculations based on such data predict three new NMMW that should result from photon pumping with isotopic CO_2 lasers. The predicted outputs lie in atmospheric windows between 0.7 and 1 mm.

Spectroscopy of D_2O

Heavy water is an important NMMW and SMMW molecule because when the D_2O gas pumped with a TEA CO_2 laser, kilowatts of output power result (10). By using heterodyne techniques, we have measured the frequencies of several D_2O absorption lines that are nearly coincident with CO_2 emission lines.

Table III presents the results of measurements of eight absorption lines in D_2O gas (14). Our measurements were taken with D_2O gas pressures from 0.1 to 0.5 torr. The line $6_6 \rightarrow 5_4$, $6_5 \rightarrow 5_5$ was studied at pressures less than 0.01 torr but was still unresolved. The line assignments are labeled according to the asymmetric top model (9). These results are being used by researchers at two universities in calculations of the efficiency of the D_2O NMMW and SMMW source.

Table III. D_2O Absorption Frequencies

D_2O Absorption[a]	CO_2 Frequency (cm^{-1})[b]	Measured Difference (cm^{-1}) $\nu(D_2O) - \nu(CO_2)$	D_2O Frequency (cm^{-1})
$6_6 \rightarrow 5_4, 6_5 \rightarrow 5_5$	1035.4736	−0.0393	1035.4343
$7_{-1} \rightarrow 6_{-1}$	1035.4736	+0.0185	1035.4921
$11_{-6} \rightarrow 10_{-6}$	1048.6608	+0.0399	1048.7007
$12_{-6} \rightarrow 11_{-6}$	1053.9235	+0.0262	1053.9497
$10_{-8} \rightarrow 9_{-6}$	1073.2785	−0.0188	1073.2597
$5_0 \rightarrow 4_0$	1079.8523	+0.0109	1079.8632
$5_0 \rightarrow 4_0$	1079.8523	+0.0106[c]	1079.8629
$10_{-7} \rightarrow 10_{-9}$	1084.6351	+0.0217	1084.6568
$9_{-9} \rightarrow 8_{-7}$	1085.7654	−0.0196	1085.7458

[a] From Ref. (7).

[b] From Ref. (15).

[c] From Ref. (16).

Spectroscopy of CH_3OH

Methyl alcohol provides more NMMW and SMMW transitions than any other molecule (10). Its structure corresponds to a slightly asymmetric top, and the vibrational transition of interest for optical pumping is the ν_4 vibration associated with the C-O stretch. The complexity introduced by the reduced symmetry is compounded by a torsional motion of the O-H group. Fig. 11 shows a comparison of the diffuse structure of the conventional spectrum (insert) and the R(5)-multiplet as obtained with the diode laser. It is also inform-

ative to compare the conventional spectrum in this figure with that of CH_3F in Fig. 2 to see how one extra atom drastically complicates molecular spectra corresponding to similar vibrations.

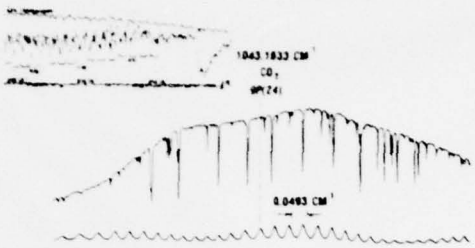

Fig. 11. Diode laser scan of ν_4, R(J = 5) multiplet in CH_3OH.

The identification of R and P multiplets was made only after hundreds of data runs of spectra were taken and fitted together. This piecewise procedure was necessitated because the tuning behavior of the diode laser made it difficult to obtain continuous spectral runs over ranges exceeding 1 cm^{-1}. Multiplets have been identified extending from the R(11) near 1052 cm^{-1} through the Q branch to the P(10) near 1017 cm^{-1}. Assignments of the torsional quantum numbers η and τ and the rotational quantum numbers J and K for certain lines in the P and R multiplets have been made possible because of the constant width of the multiplets, the similarity of the structures of adjacent multiplets, and our Stark measurements. Lines in the P and R branch of the ν_4 band with $J \leq 2$ were identified by direct observation in absorption of the Stark patterns produced when the static E-fields were applied to the gas with $\vec{E}$ either parallel or perpendicular to the linear polarization of the diode laser radiation. The K-values could be unambiguously assigned since the K = 0 lines showed no resolvable Stark splitting, whereas other lines showed well resolved linear or quadratic Stark effects. Fig. 12 shows the quadratic Stark effect on the R(J = 1, η = 0, K = 1, τ = 3) asymmetry-split pair of lines. The agreement between the measured splitting of 214 MHz and our theoretical calculation of 195 MHz is within our experimental uncertainty of 30 MHz. This result allows us to make an unambiguous quantum number assignment for these lines. An example of a linear Stark splitting is shown in Fig. 8. By superimposing the various R(J) multiplets, by using the heterodyne results, and by comparing the similarities of structure, we have given an absolute frequency scale to the CH_3OH spectrum and have established the identifications of the K-values in the multiplet as shown schematically in Fig. 13. The assignments for the J = 0, 1, and 2 multiplets are confirmed by Stark spectra, and the assignments in the higher J multiplets are extrapolations from frequency and intensity considerations.

From our data, it was possible to make definitive tests of two published theoretical calculations (17, 18) which attempted to identi-

*SATTLER, WORCHESKY, RITTER,
SIMONIS, & RIESSLER

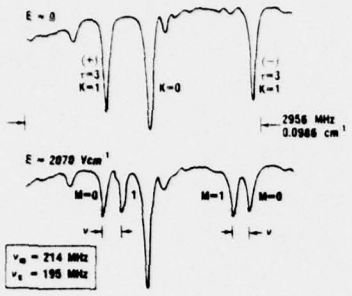

Fig. 12. Quadratic Stark effect on ν_4, $R(J = 1, \eta = 0, \tau = 3\ K = 1)$ pair in CH_3OH.

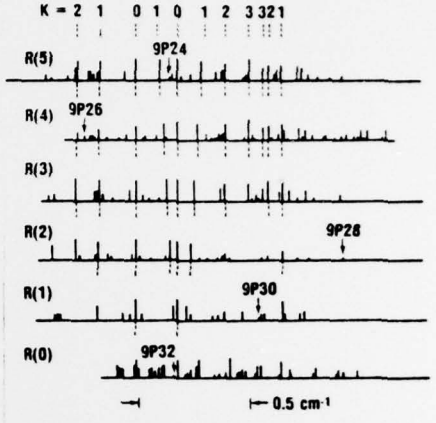

Fig. 13. Schematic spectra of ν_4, $R(J)$-multiplets.

fy the IR and NMMW-SMMW transition. The results of heterodyne spectroscopy for pumping CH_3OH with the CO_2 9P16 line is shown in Fig. 14. A strong CH_3OH line lies within 105 MHz of the CO_2 laser frequency. This pumping frequency has produced four NMMW transitions and one SMMW transition, including the important line at 1.217 mm (10). Additional measurements place the offset at 73 ± 15 MHz. These data, when combined with the analysis of the structure of the $R(J \approx 10)$ multiplets, lead to an identification of the strong absorption line as the higher frequency $R(J = 10, \eta = 0, \tau, K = 0)$ transition in partial agreement with Ref. (17) and in disagreement with the conclusion of Ref. (18). Similar methods also show that the assignment as an $\eta = 1$ transition (17) for the IR absorption in the Q branch associated with pumping by the 9P34 line may not be correct since a strong $\eta = 0$ line lies close to the laser frequency.

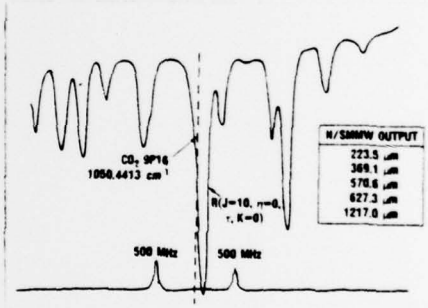

Fig. 14. Heterodyne spectroscopy of ν_4, $R(J = 10, K = 0)$ transition in CH_3OH.

From the etalon and heterodyne spectroscopy and the published frequencies of isotope CO_2 lasers, it has been possible to predict a near-coincidence of an $R(J = 6, \eta = 0, \tau, K = 3)$ line with the IIP48 line of the CO_2^{18} laser. Calculations are proceeding to predict also

the resultant NMMW and SMMW output frequencies.

Conclusions

New IR heterodyne and Stark spectroscopic techniques have been developed and applied to the analysis of molecular NMMW sources. These procedures have revealed previously unresolved molecular IR structure. Quantum number assignments and absolute frequencies of transitions have been tabulated for CH_3F, D_2O, and CH_3OH. New NMMW operating frequencies have been predicted. The results have implications for both fundamental and applied research, since our measurements provide new information regarding molecular structure, as well as important parameters for NMMW source modeling.

Acknowledgements

The authors thank T. DeTemple of the University of Illinois for suggesting D_2O as a gas for study and J. Gallagher of the Georgia Institute of Technology for suggesting the application of Stark fields.

References

1. Near-Millimeter Wave Technology Base Study, S. M. Kulpa and E. A. Brown, eds., U.S. Army Electronics Research and Development Command, Harry Diamond Laboratories (in press).
2. W. L. Smith and I. M. Mills, J. Mol. Spectrosc. II, 11 (1963).
3. W. H. Weber and P. D. Maker, J. Chem. Phys. 64, 2149 (1976).
4. R. S. Eng et al., Mol. Phys. 28, 653 (1974).
5. E. D. Hinkley, Appl. Phys. Lett. 16, 351 (1970).
6. T. W. Meyer, Ph.D. Thesis, U. Cal. Livermore (1974).
7. C. L. Lin and J. H. Shaw, 31st Molecular Spectroscopy Symposium, FC10, Columbus, Ohio (1976).
8. S. M. Freund et al., J. Mol. Spectrosc. 52, 38 (1974).
9. C. H. Townes and A. L. Schawlow, "Microwave Spectroscopy," McGraw-Hill, New York (1955).
10. M. Rosenbluh et al., Appl. Opt. 15, 2635 (1976).
11. J. P. Sattler and G. J. Simonis, J. Quant. Elect. 13, 461 (1977).
12. G. Hertzberg, "Molecular Spectra and Molecular Structure," Vol. II, Van Nostrand, New York (1945).
13. R. S. Winton and W. Gordy, Phys. Lett. 32A, 219 (1970).
14. T. L. Worchesky et al., Opt. Lett. (in press).
15. F. R. Petersen et al., Proceedings on Laser Spectroscopy, Vail, Colorado, 1973, Plenum, New York (1974).
16. F. Keilman et al., Appl. Phys. Lett. 26, 19 (1975).
17. J. O. Henningsen, J. Quant. Elect. 13, 435 (1977).
18. E. J. Danielewicz, Jr., and P. Coleman, J. Quant. Elect. 13, 485 (1977).